Species-Area Curves, Diversity Indices, and Species Abundance Distributions: A Multifractal Analysis

Luís Borda-de-Água,[1,*] Stephen P. Hubbell,[2,†] and Murdoch McAllister[3,‡]

1. Center for Environmental Research and Conservation, Columbia University, New York, New York 10027;
2. Department of Botany, University of Georgia, Athens, Georgia 30602; and Smithsonian Tropical Research Institute, Box 2072, Balboa, Panama;
3. Department of Environmental Science and Technology, Imperial College, Room 4.89, Royal School of Mines, Prince Consort Road, London SW7 2BP, United Kingdom

Submitted May 15, 2000; Accepted June 8, 2001

ABSTRACT: Although fractals have been applied in ecology for some time, multifractals have, in contrast, received little attention. In this article, we apply multifractals to the species-area relationship and species abundance distributions. We highlight two results: first, species abundance distributions collected at different spatial scales may collapse into a single curve after appropriate renormalization, and second, the power-law form of the species-area relationship and the Shannon, Simpson, and Berger-Parker diversity indices belong to a family of equations relating the species number, species abundance, and area through the moments of the species abundance–probability density function. Explicit formulas for these diversity indices, as a function of area, are derived. Methods to obtain the multifractal spectra from a data set are discussed, and an example is shown with data on tree and shrub species collected in a 50-ha plot on Barro Colorado Island, Panama. Finally, we discuss the implications of the multifractal formalism to the relationship between species range and abundance and the relation between the shape of the species abundance distribution and area.

Keywords: species-area relationship, species diversity indices, species abundance distribution, multifractals, method of moments, method of histograms.

One of the best-known patterns in ecology is the power-law form of the species-area relationship

$$S(A) = cA^z, \tag{1}$$

where $S(A)$ is the number of species in a taxonomic group within area A, and c and z are constants. Such a general pattern is important not only for fundamental aspects of ecological theory but also for ecological applications such as the design of reserves (e.g., Gilpin and Diamond 1980; Higgs and Usher 1980) and the estimation of species extinction rates (e.g., May et al. 1995; Pimm et al. 1995). For a recent comprehensive review of species-area relationships, see Rosenzweig (1995).

According to Rosenzweig (1995), a species-area relationship (hereafter SAR) of the form of equation (1) was first suggested by H. C. Watson in the first half of the nineteenth century for the vascular plant species of Great Britain. A similar study with similar conclusions was reported by Arrhenius (1921) for the plant communities of islands of Stockholm, Sweden. Since then, ecologists have attempted to derive the power-law SAR from statistical sampling theories (e.g., Preston 1962; MacArthur and Wilson 1967; May 1975; Caswell and Cohen 1993) or dynamical theories (Hubbell 1997, 2001). Preston (1962) and May (1975) sought to derive the power-law SAR from the assumption that the species abundance distribution of a taxonomic group is described by a lognormal distribution. These authors showed that, under certain assumptions, the value of the exponent z is approximately equal to 0.25, a value frequently found for SARs for taxa on islands of the same archipelago but larger than the values frequently estimated for nested areas within an island or a continent, where $z \approx 0.12$ (e.g., Rosenzweig 1995).

More recently, attention has shifted to simulation studies, which attempt to elucidate the underlying biological factors that might determine the shape of SAR curves and the slopes (z values) that are empirically observed (Durrett and Levin 1996; Leitner and Rosenzweig 1997; Ney-Nifle and Mangel 1999; Pelletier 1999; Hubbell 2001). Some of these studies have challenged Preston's (1962) and May's (1975) findings. Leitner and Rosenzweig (1997) and Pelletier (1999) showed that the z values obtained by simulations with only the assumptions used in Preston's (1962)

* E-mail: bdagua@ldeo.columbia.edu.

† E-mail: shubbell@dogwood.botany.uga.edu.

‡ E-mail: m.mcallister@ic.ac.uk.

Am. Nat. 2002. Vol. 159, pp. 138–155.

and May's (1975) theory always substantially exceeded those predicted by the theory or those empirically observed. In order to obtain z values close to the observed ones, an extra assumption concerning species range size and abundance had to be introduced.

Durrett and Levin (1996) and Hubbell (1997, 2001) took another approach. They assumed that SARs are dynamic and reflect a spatial diversity equilibrium among the ongoing processes of speciation, dispersal, and extinction on a biogeographic landscape. Durrett and Levin (1996) showed that z values depend on the speciation rate, and Hubbell (1997, 2001) showed that they also depend on the dispersal rate of species over the landscape relative to the speciation rate.

Instead of trying to derive the power-law form of the SAR from basic principles, Harte and Kinzig (1997) derived several ecological consequences by simply assuming that equation (1) holds. In particular, Harte and Kinzig (1997) pointed out that, as a power law, equation (1) implies self-similarity in the relation between the number of species and area. The concept of self-similarity is commonly found in the study of fractals, where it is a main characteristic of some, but not all, fractal objects or signals (for the application of fractals in ecology, see, e.g., Hastings and Sugihara 1993). Self-similarity is defined as follows: given any two areas A_1 and A_2, as long as the ratio A_1/A_2 is constant, the ratio of the number of species found in A_1 and A_2, $S(A_1)/S(A_2)$, is constant, independent of the spatial scale at which the areas are chosen. In other words, the same pattern is observed at different spatial scales. In nature, however, self-similarity is expected to be observed only within a certain intermediate range of areas (Hubbell 2001), not at all spatial scales, as assumed by Harte et al. (1999). At small spatial scales, the SAR relationship is not governed by equation (1) but is curvilinear on a log-log plot, and at large scales, the SAR bends upward toward a limiting slope of unity (Durrett and Levin 1996; Hubbell 2001).

It is often the case that when a fractal is observed a more general class of self-similar relations called "multifractals" (to be defined later) also exists (e.g., Mandelbrot and Evertsz 1996). In contrast to a fractal object, or signal, where a single number (called its "dimension") is sufficient for complete characterization, a multifractal requires an infinite number of indices, frequently called "a spectrum." Multifractals are mainly a probabilistic concept. Two main methodological approaches have dominated the study of multifractals (Evertsz and Mandelbrot 1992). One focuses on the moments of the underlying distribution function (the method of moments) and the other on the distribution function directly (the histogram method). (For examples of application of multifractals in ecology, see, e.g., Pascual et al. 1995 and Manrubia and Solé 1996.)

In this article, we apply the multifractal approach to studying SARs. We assume a spatial scale on which the power-law SAR relationship applies. Adopting the multifractal approach allows us to extend the theory of SARs beyond the simple description of species richness in a given area to include relative species abundance as well. We believe that the generalization of the power law of the SAR using the multifractal formalism is potentially far reaching. First, it ties species-area theory to a number of indices used widely to quantify diversity. Second, it generates a number of new hypotheses about patterns of biodiversity for further investigation. Third, it develops new tools for addressing practical issues such as conservation. The uncovering of deeper biodiversity patterns so far unobserved is, in our opinion, one of the main contributions of this article.

We highlight the following predictions and consequences of the multifractal formalism. The method of moments and the histogram method yield different aspects of the theory. First, the method of moments leads to power-law functional relationships between area and the Shannon, Simpson, and Berger-Parker diversity indices (Magurran 1988). To our knowledge, this is the first time that explicit relations between these diversity indices and area have been put forward. The method of moments also reveals a relationship between the fraction of individuals of a species and area, which is compatible with a widely observed pattern, namely, that very abundant species are widespread and rare species have smaller ranges (e.g., Brown 1984; Gaston et al. 1997; Hubbell 2001). Second, the histogram method allows us to study the species abundance as well and, in particular, to study the spatial evolution of the relative species abundance distribution. The histogram method shows that under the power-law SAR, the species abundance distributions, after an appropriate renormalization, converge to a limiting curve when area increases. The latter is probably the most important consequence of the application of multifractals to theoretical and practical studies.

Because multifractals are poorly known in ecology, the next section briefly reviews the main results of multifractal theory. We start with a simple example concerning the estimation of the multifractal spectrum of a set of points in a surface, a typical example of application of multifractals (e.g., Cheng and Agterberg 1995). The connection with the SAR is then established by analyzing the role of the quantities in the equation determining the fractal dimension and the power-law form of the SAR (eq. [1]). The method of moments is then developed specifically in the context of analyzing the species abundance distribution, followed by the histogram method. However, the order is interchangeable, and the reader may prefer to begin with the histogram method. We give the basic al-

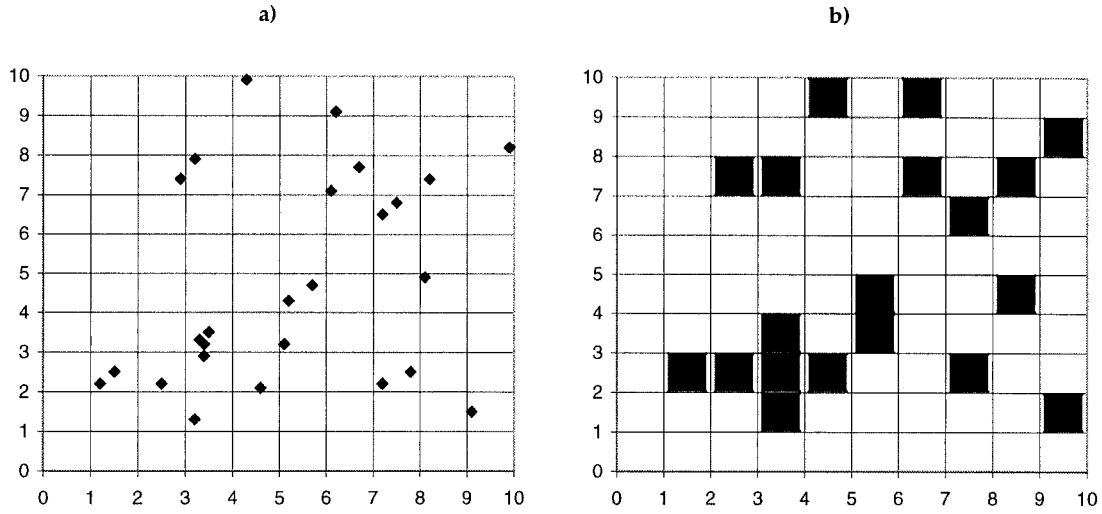

Figure 1: Example of application of the box-counting method; *a*, set of points in a square plot; *b*, squares required to cover all the points

gorithms for estimating the multifractal spectrum from raw data for both methods. Data collected for a given taxon with information on location, number, and species of individuals are suitable to the application of these methods. To exemplify the application of multifractal methods, we use data on the tree composition of a 50-ha tropical forest plot of Barro Colorado Island, Panama. The last section discusses the relevance of multifractal analysis for ecological theory in general and practical conservation issues.

The Theory of Multifractals

The theory of multifractals, as applied to patterns of relative species abundance, can take two methodological approaches. One is to construct histograms of frequency of species having a given abundance. Preston's species abundance curves are an example (e.g., Preston 1948, 1962; MacArthur and Wilson 1967; Nee et al. 1991). Another is to describe the distribution of the relative species abundance directly in terms of the moments of the sample distribution. These two approaches lead to two different methods of determining the multifractal spectrum: the method of histograms and the method of moments (Evertsz and Mandelbrot 1992), respectively. Each of these methods imposes different necessary and sufficient criteria for a distribution to be multifractal; the method of moments is more stringent, and distributions that pass the criterion of this method will be called "restricted multifractal distributions." We first explain in detail the method of moments, followed by the histogram method, before considering a practical example.

The Method of Moments

Fractal Dimensions and SARs. One of the most popular techniques used in conjunction with the method of moments is the so-called box-counting algorithm. An example of application of this method in ecology (only for fractal sets, not multifractals) is given by Morse et al. (1985). The method consists of covering an object with a set of boxes (squares, if the object is embedded in a two dimensional space) of linear size ε and counting how many boxes contain at least one point. Call the number of occupied boxes $N(\varepsilon)$. Figure 1 exemplifies the box-counting method for a set of points in a plane. Figure 1*b* shows the boxes with a certain size ε required to cover the set of points of figure 1*a*. The same procedure is then repeated for boxes with different sizes. If an object is a fractal, then a dimension D_0 (the reason for the subscript will be made clear soon), called the "box-counting dimension," is formally defined as

$$D_0 = \lim_{\varepsilon \to 0} -\frac{\log (N(\varepsilon))}{\log (\varepsilon)}. \quad (2)$$

In real applications, for obvious reasons, the limit cannot be attained, and instead, we require only that within a certain range of values of ε, called the "scaling region," the number of boxes follows a power law such that

$$N(\varepsilon) \propto \varepsilon^{-D_0}. \quad (3)$$

In practice, log-log plots are used, and the scaling region is defined as the range where a straight line is observed.

The fractal dimension is estimated as the slope of this line. A caveat is in order at this point: there are no theoretically defined rules to determine the scaling region or regions if more than one is identified. Except for some mathematically constructed deterministic fractals, in general, the scaling region must be empirically determined. This situation is not unlike the choice of the scaling region where a SAR follows, approximately, a linear relation in a log-log plot.

We can easily establish how the power-law form of the SAR (eq. [1]) is related to the estimation of the fractal dimension (eq. [3]) since they are both power laws. If equation (1) is written in the form

$$S(A) \propto \left(\frac{1}{A}\right)^{-z},$$

then the number of species, $S(A)$, plays the same role as the total number of boxes, $N(\varepsilon)$, with $1/A$ as ε, and z as D_0.

The Partition Function and the Spectrum of Generalized Exponents. So far, only the presence or absence of points in a box has mattered; information on the relative number of points inside each box has not been used. For some fractals, called "homogeneous fractals," or "monofractals," all boxes contain the same number of points. For other fractals, called "heterogeneous fractals," or "multifractals," the number of points inside boxes are different, and the relative point abundances among boxes have distributional scaling properties with ε that are themselves self-similar on different spatial scales.

In order to characterize a multifractal using the method of moments, the so-called partition function, χ_q, is defined as

$$\chi_q(\varepsilon) = \sum_{i=1}^{N(\varepsilon)} p_i^q, \tag{4}$$

where p_i is the proportion of the points falling inside box i and q is a chosen (positive or negative) real number. To understand the origin of the designation "method of moments," observe that equation (4) can also be written as

$$\chi_q(\varepsilon) = \sum_{j=p_{\min}}^{p_{\max}} p_j^q F(p_j). \tag{5}$$

Equation (4) is summed over the set of all individual boxes, whereas equation (5) is summed over categories of abundance p, and $F(p_j)$ is the frequency of boxes with abundance p_j. Notice that $\chi_q(\varepsilon)/N(\varepsilon)$ corresponds to the definition of the qth moment of the $F(p_j)$. Clearly, the numerical value of the sum in equations (4) and (5) depends on the size of the exponent q; that is, they depend on which moment is selected.

The importance of q, among other things, is that different values of this variable allow the theory to generate many of the well-known indices of diversity, as we will demonstrate below. Mathematically, the variable q determines the sensitivity of equations (4) or (5) to high- or low-abundance boxes. That is, depending on the choice of q, boxes with different p_i give different contributions to the sum in equation (4) or (5). When q is a large positive number, the main contribution to the sum comes from the largest p_i, and the term corresponding to the smallest p_i is negligible. However, when q is a very small negative number (large in absolute value), p_i^q for large p_i becomes negligible relative to the contribution of the smallest p_i. The following example illustrates the role of q. Imagine that there are only two p_i, $p_1 = 0.75$ and $p_2 = 0.25$. If $q = -10$, $p_1^{-10} = 17.76$ and $p_2^{-10} = 1{,}048{,}576$; that is, the contribution of p_1 is negligible. Conversely, if $q = 10$, $p_1^{10} = 0.056$ and $p_2^{10} = 9.54 \times 10^{-7}$, it is now the contribution of p_2 that can be neglected.

A description of a multifractal is obtained by defining the generalized (box-counting) dimensions, also called "Rényi dimensions" (e.g., Grassberger 1983):

$$D_q = \lim_{\varepsilon \to 0} \frac{1}{q-1} \frac{\log\left(\sum_{i=1}^{N(\varepsilon)} p_i^q\right)}{\log(\varepsilon)} = \lim_{\varepsilon \to 0} \frac{1}{q-1} \frac{\log(\chi_q)}{\log(\varepsilon)}. \tag{6}$$

The spectrum of generalized dimensions, D_q, has a sigmoidal-shaped curve and is a monotonically decreasing function of q (e.g., Grassberger 1983). Recalling the previous discussion on the role of q, we note that D_q reflects the characteristics of the less dense regions of the set of points when $q < 0$, and it reflects the denser regions when $q > 0$.

Returning to the power-law form of the SAR, we define a partition function, $\chi_q(A)$, in terms of the relative number of individuals of a given species i; $p_i = n_i/N$, where n_i is the number of individuals of species i, and N is the total number of individuals of all species:

$$\chi_q(A) = \sum_{i=1}^{S(A)} p_i^q. \tag{7}$$

The sum is now performed over all the species, $S(A)$, within area A. Making use of the previous analogy between $1/A$ and ε and $S(A)$ and $N(\varepsilon)$, we introduce an equation equivalent to equation (6) that we call the spectrum of generalized exponents:

$$z_q = \lim_{A\to\infty} \frac{1}{q-1} \frac{\log\left(\sum_{i=1}^{S(A)} p_i^q\right)}{\log(1/A)},$$

or

$$z_q = \lim_{A\to\infty} \frac{1}{1-q} \frac{\log\left(\sum_{i=1}^{S(A)} p_i^q\right)}{\log(A)} = \lim_{A\to\infty} \frac{1}{1-q} \frac{\log(\chi_q)}{\log(A)}. \quad (8)$$

In the same way the D_q spectrum characterized a multifractal object, the z_q spectrum characterizes a multifractal species abundance distribution. The observations previously made about the shape of the D_q spectrum and the role of the parameter q also apply to the z_q spectrum: z_q has a sigmoidal shape, and it is a monotonically decreasing function of q. When q is a large positive number, the most abundant species are selected, and when it is a small negative number, the rarest species are selected. The significance of the values of z_q for the scaling of p_i with A will be discussed in detail later.

In practical situations, clearly, the limit $A \to \infty$ in equation (8) cannot be attained. In order to determine z_q, one should investigate whether plots of $\log(\sum_{i=1}^{S(A)} p_i^q)$ versus $\log(A)$ for several values of q are straight lines within a certain range of area A. (Note: $q = 1$ is a special case that we will discuss later.) In other words, power-law relations should be observed not only for the relation between the number of species and A but also for the moments of the relative abundance of species and A. We stress the importance of choosing the upper and lower limits of the scaling region carefully because power laws may not be a good description for all spatial scales or more than one scaling region may be present.

The z_q Spectrum and Species Diversity Indices. As previously mentioned, the methods of moments lead to functional relations between some well-known diversity indices and area A. These can be obtained from equation (8) for selected values of q. Formulas for $q = 0, 1, 2$ and the limiting cases $q \to \pm\infty$ are given explicitly below.

When $q = 0$, the familiar power-law form of the SAR is recovered:

$$z_0 = \lim_{A\to\infty} \frac{\log(S(A))}{\log(A)}. \quad (9)$$

For $q = 1$, equation (8) cannot be solved since the denominator becomes 0. The solution is to take the limit $q \to 1$ and apply the l'Hôpital rule. The result is

$$z_1 = \lim_{A\to\infty} \frac{-\sum_{i=1}^{S(A)} p_i \log(p_i)}{\log(A)}, \quad (10)$$

where the Shannon's index can be recognized in the numerator.

For $q = 2$, one obtains, by simple substitution of q by 2,

$$z_2 = -\lim_{A\to\infty} \frac{\log\left(\sum_{i=1}^{S(A)} p_i^2\right)}{\log(A)}, \quad (11)$$

where the numerator corresponds to the logarithm of the Simpson's index.

In the limiting case $q \to \infty$, the sum in equation (8) is dominated by the largest value of p, $p_{\max}$, then becoming

$$z_\infty = -\lim_{A\to\infty} \frac{\log(p_{\max})}{\log(A)}, \quad (12)$$

where $p_{\max}$ is the Berger-Parker index (e.g., Magurran 1988).

Contrarily, for $q \to -\infty$, the sum is dominated by the smaller p, $p_{\min}$, and one obtains

$$z_{-\infty} = -\lim_{A\to\infty} \frac{\log(p_{\min})}{\log(A)}. \quad (13)$$

Hill (1973) noted that some of these indices could be derived from a single formula, the generalized entropy of order q, first introduced by Rényi (1961), which is, in fact, the term

$$\frac{1}{1-q} \log\left(\sum_{i=1}^{S(A)} p_i^q\right)$$

in equation (8). What is discovered here is that equations (10)–(12) indicate that a functional relation with area exists for the Shannon, the Simpson, and the Berger-Parker indices. Specifically, equation (10) implies that when the Shannon index is plotted as a function of $\log(A)$, a straight line with slope z_1 is obtained, and equations (11) and (12) imply that the Simpson and the Berger-Parker indices exhibit a power-law relationship with the area such as A^{-z_2} and $A^{-z_{+\infty}}$, respectively; that is, when plotted as a function of A in a log-log plot, straight lines with slopes $-z_2$ and $-z_{-\infty}$ are observed.

Some Extreme Cases. Analysis of equation (8) in some

special cases leads to the extreme values of z_0 and clarifies the interpretation of z_0. Suppose all species are equally abundant, each with the same number of individuals, such that for a given area, all p_i is constant. In this case, the sum in equation (8) reduces to $S(A)^{(1-q)}$ and

$$z_q = z_0 = \lim_{A\to\infty} \frac{\log(S(A))}{\log(A)},$$

that is, the z_q are all the same and independent of q (this is the equivalent to a homogeneous fractal).

Consider now two extreme situations that lead to different and extreme values of z_0. Species may or may not have the same number of individuals. First, all species are spatially, perfectly, and uniformly distributed. In this case, one can define a minimum area, A_m, within which all species are represented by at least one individual. Then, for any area larger than A_m, no more new species will be found, which implies a constant value for S. Since z_0 is defined in the limit of $A \to \infty$, this situation implies $z_0 = 0$. In the second extreme case, each species is found only in one contiguous region. Assume also that each species occupies the same area. If this is the minimum area of sampling, the number of species, S, will increase linearly with A, then $z_0 = 1$. The latter situation corresponds to a case of complete spatial independence of regional biogeographical processes (Durrett and Levin 1996).

Observe that, in these two extreme cases, there were no restrictions on the shape of the distribution of species abundance, which shows that the same distribution may imply different values of z, depending on the spatial distribution of species over the landscape or that different species abundance distributions may lead to the same value of z. This seems to contradict the argument of Harte et al. (1999) who derive a one-to-one functional mapping between z and a unique species abundance distribution of a given region. This happened because, at the smallest scale, the species distribution was always the same, although, in the same article, Harte et al. (1999) make some provisions for the cases where the power-law relationship breaks down, in particular, for small areas. In practical situations, the limit of validity of the power-law SAR is restricted to a certain range of areas, and a different species distribution at the lower limit of the of the SAR power-law region may lead to different species distributions at larger areas even if the same exponent z is observed.

An Algorithm for the Method of Moments. A basic iterative process to obtain z_q from raw data, which consists of the relative species abundance of a given taxon within a certain area.

Step 1. For a given area, A, compute the partition function $\chi_q(A)$ (eq. [7]).

Step 2. Repeat the previous step for areas of different sizes.

Step 3. Plot $\log(\chi_q)$ versus $\log(A)$ for different values of q, and check whether the lines are straight.

Step 4. If the lines are straight, then compute the slope τ_q; z_q is obtained from $z_q = \tau_q/(1 - q)$. As discussed before, $q = 1$ is a special case, and instead of the partition function, take $-\sum_{i=1}^{S(A)} p_i \log(p_i)$ versus $\log(A)$.

The following very simple example shows explicitly the numerical steps to obtain the z_q spectrum. Consider two areas, A_1 and A_2, such that $A_2 = 2A_1 = 20$ (arbitrary units). Area A_1 has five species from a given taxon with a total number of individuals, $N_T = 105$, distributed by species as $n = (1, 3, 25, 26, 50)$. Area A_2 contains the previous species plus a new one and $N_T = 210$, distributed by species as $n = (1, 5, 48, 50, 98, 8)$. For area A_1, $p_i = n_i/N_T = (0.0095, 0.0286, 0.238, 0.248, 0.476)$, and for A_2, $p_i = (0.0048, 0.0238, 0.228, 0.238, 0.467, 0.038)$. For the sake of simplicity, we consider only $q = -2$ and 2. For $q = -2$, the value of the partition function obtained from application of equation (7) is $\chi_{-2}(A_1) = 12{,}288.36$ and $\chi_{-2}(A_2) = 46{,}594.43$, or $\log(\chi_{-2}(A_1)) = 4.089$ and $\log(\chi_{-2}(A_2)) = 4.668$. For $q = 2$, $\chi_2(A_1) = 0.34567$ and $\chi_2(A_2) = 0.32875$, or $\log(\chi_2(A_1)) = -0.4613$ and $\log(\chi_2(A_2)) = -0.4831$; these calculations correspond to steps 1 and 2. In a real situation, where more areas are sampled, step 3 requires a check of the linearity of $\log(\chi_q)$ versus $\log(A)$. In our simple example, the slopes of $\log(\chi_q)$ versus $\log(A)$ are $\tau_{-2} = 1.92$ and $\tau_2 = -0.07$ and from equation (8), $z_{-2} = 0.64$ and $z_2 = 0.07$. Application of these steps for more values of q would allow us to draw the spectrum of generalized exponents, z_q.

Step 3 suggests a definition of a multifractal distribution: a distribution is called "multifractal" if power-law relationships of $\chi_q(A)$ exist for all q. This is the crucial aspect of the method of moments. If the lines are not straight, then the method is not applicable. However, even if the lines are not straight for all values of q, the distribution may still be self-similar. Mandelbrot and Evertsz (1996) showed that there are exactly self-similar distributions for which the method of moments fails to apply. Two situations were identified: straight lines are not observed for negative q's below a certain q_{bottom} or for positive q's above a certain q_{top}. The former case occurs when, for some i, p_i^q tends to 0 with A faster than any power law, and the latter occurs when p_i^q tends to 0 with A slower than any negative power law, $A^{-\alpha}$ (see Mandelbrot and Evertsz 1996 for details). Self-similar distributions to which the method of moments can be applied are called "restricted multifractals" to distinguish them from a more general class of multifractal distributions for which not all moments exist. In the cases where the method of moments cannot be

applied, one has to resort to the histogram method (Mandelbrot and Evertsz 1996).

The Histogram Method

The histogram method, also called the "method of distributions" (Mandelbrot and Evertsz 1996), is an alternative to the method of moments of characterizing a multifractal distribution. This method deals directly with the distribution function, instead of the moments, so we can still, in principle, estimate the multifractal spectrum in cases where the method of moments fails. The method starts by constructing histograms of the relative species abundance distribution for areas of different size, followed by some appropriate transformations, as described below. For the reader interested in more detailed theoretical explanations of this method, the reviews by Evertsz and Mandelbrot (1992) and Mandelbrot and Evertsz (1996) are highly recommended.

The Spectrum of Scaling Indices, f(α). While the method of moments led to the z_q spectrum, the histogram method leads to the spectrum of scaling indices, $f(\alpha)$. In the practical situations dealt with in this article, α is the so-called coarse Hölder exponent, or simply Hölder exponent, and plays a central role in this method. It is defined as

$$\alpha_i = -\frac{\log(p_i)}{\log(A)}, \tag{14}$$

where p_i is, as before, the relative abundance of species *i.* Since p_i is smaller than 1, and we are interested in the limit $A \to +\infty$, the negative sign guarantees that α is a positive number. Observe that the largest value of α, $\alpha_{\max}$, is achieved when $p_i = p_{\min}$, which corresponds to the rarest species, and conversely, the smallest α, $\alpha_{\min}$, is obtained when $p_i = p_{\max}$, the most abundant species; notice that comparison of equation (14) with equations (12) and (13) allows us to conclude that, in the limit of very large areas, $\alpha_{\max} = z_{-\infty}$ and $\alpha_{\min} = z_{+\infty}$.

To obtain the $f(\alpha)$ spectrum, the first step consists of determining, for a given area, A, how many species, S_α, have the same Hölder exponent, α. These values are then grouped into "bins" to produce a histogram. The curves of S_α versus α are very similar to the Preston species abundance curves. The main difference between the S_α curves and Preston curves is that the logarithms are of the fractional relative abundance on the *X*-axis, further normalized by area, that is, $\log(p_i)$ divided by $\log(A)$, according to equation (14).

We are interested in the limit when $A \to +\infty$. Clearly, one expects $S_\alpha(A)$ to be different when area A increases. As typically occurs in the study of fractals, we are interested in an intrinsic characteristic that remains constant independently of the independent variable, in this case area A. That characteristic can be found by rescaling or renormalizing to prevent the limit to diverge. In this article, we explore a renormalization of the form $f_A(\alpha) = \log(S_\alpha(A))/\log(A)$ (Evertsz and Mandelbrot 1992). The spectrum of the scaling indices, $f(\alpha)$, is then defined as

$$f(\alpha) = \lim_{A\to\infty} \frac{\log(S_\alpha(A))}{\log(A)}. \tag{15}$$

This renormalization and the existence of the limit in equation (15), which we stated here without proof, are consequences of the Harald Cramér theorem on large deviations (see Evertsz and Mandelbrot 1992 for details).

Once again, the limit cannot be found, but we can observe the preasymptotic behavior of equation (15) as area becomes larger. Mandelbrot and Evertsz (1996) call these curves "preasymptotic $f_A(\alpha)$" in order to distinguish from $f(\alpha)$, which is the limiting curve. If the $f_A(\alpha)$ curves collapse into a single one, $f(\alpha)$, then the distribution is said to be multifractal.

Often, the shape of the $f(\alpha)$ spectrum is similar to the mathematical symbol $\cap$ (see appendix), where the minima correspond to the values of $f(\alpha_{\min})$ and $f(\alpha_{\max})$, and possibly lean to one side. In some cases, however, the portion of the $f(\alpha)$ spectrum to the right of the maximum is a straight line with a constant value equal to $f_{\max}(\alpha)$ and $\alpha_{\max} = +\infty$. In this case, because the left side of the spectrum has the same shape as before, the multifractal distribution is called a "left-sided multifractal" (Mandelbrot and Evertsz 1996). For such multifractals, the moments are not defined for $q < q_{\text{bottom}} < 0$ (one of the situations, previously mentioned, where the method of moments fails). This fact has led some authors to call these multifractals "anomalous multifractals" (e.g., Paladin and Vulpiani 1987). Another anomalous-situation case occurs when $\alpha_{\min} = 0$. In this case, the overall shape is still like $\cap$, but the $f_{\max}(\alpha)$ spectrum reaches $\alpha = 0$. When this happens, the moments are not defined for $q < q_{\text{top}} < 0$, and again, the method of moments cannot be applied, as already pointed out (Mandelbrot and Evertsz 1996).

The Relation between the f(α) *and the* z_q *Spectrum.* When the moments of the distribution function exist, the z_q and the $f(\alpha)$ spectra can be related. In this case, the calculation of $f(\alpha)$ is easier with the method of moments, and the relation of z_q and $f(\alpha)$ can be established through a Legendre transformation. The derivation of the formulas relating the two spectra is well known (Halsey et al. 1986) and is shown for this study in the appendix. The Legendre

transformation is given by the following pair of equations:

$$f(\alpha(q)) = (1 - q)z_q + q\alpha(q), \tag{16a}$$

$$\alpha(q) = z_p - (1 - q)\frac{dz_q}{dq}, \tag{16b}$$

where $\alpha(q)$ is the value of α corresponding to the p_i that gives the main contribution to the partition function, χ_q, for a selected value of q.

An Algorithm for the Histogram Method. The basic steps to compute the $f(\alpha)$ spectrum from a data set are as follows:

Step 1. For a given area A, determine for each species the Hölder exponent, as defined by equation (14).

Step 2. Divide the range of α into equal bins, $\Delta\alpha$, and count the number of occurrences (species) in each bin, S_b; the correspondent S_α is equal to $S_b/\Delta\alpha$.

Step 3. Draw the histogram of $\log(S_\alpha)/\log(A)$ versus $\log(\alpha)$, the $f_A(\alpha)$ curve.

Step 4. Repeat the previous steps for areas of different sizes, A. If the distribution is multifractal, then the curves of $\log(S_\alpha)/\log(A)$ versus $\log(\alpha)$ should collapse into a single curve when $A \to \infty$.

As with the method of moments, we show the application of the histogram method to the same numerical example. Once the p_i are calculated, α can be calculated using equation (14). For A_1, $\alpha(A_1) = (2.02, 1.54, 0.62, 0.61, 0.32)$, and for A_2, $\alpha(A_2) = (1.78, 1.25, 0.49, 0.48, 0.254, 1.09)$. If $\Delta\alpha = 0.25$, and if we take nine bins, then for A_1, the number of species, S_b, in bin]0.25, 0.5] is one, in bin]0.5, 0.75] is two, in bin]1.5, 1.75] is one, and in bin]2.0, 2.25] is one. For A_2, the number of species in bin]0.25, 0.5] is three, in bin]1.0, 1.25] is two, and in bin]1.75, 2.0] is one. Finally, calculating $S_\alpha = S_b/\Delta\alpha$, for A_1, $f_A(\alpha) = \log(S_\alpha)/\log(A_1)$, the number of species in bin]0.25, 0.5] is 0.602, in bin]0.5, 0.75] is 0.903, in bin]1.5, 1.75] is 0.602, and in bin]2.0, 2.25] is 0.602. For A_2, $f_A(\alpha) = \log(S_\alpha)/\log(A_1)$, the number of species in bin]0.25, 0.5] is 1.079, in bin]1.0, 1.25] is 0.903, and in bin]1.75, 2.0] is 0.602.

The convergence to a limiting curve, as required by step 4, is the counterpart of the power-law scaling required in the method of moments (step 3). According to Evertsz and Mandelbrot (1992, p. 942), the method of moments converges faster because the calculation of the moments tends to smooth the data, whereas the histogram method deals with the raw data. Although the histogram is more generally applicable, the convergence to $f(\alpha)$ can be extremely slow. On the other hand, the method of moments is not of general applicability because the moments may fail to have power-law behavior as a function of area. However, when it can be used, it leads to a faster convergence than the method of histograms, and the z_q spectrum is related to the $f(\alpha)$ spectrum through a Legendre transformation (eqq. [16]).

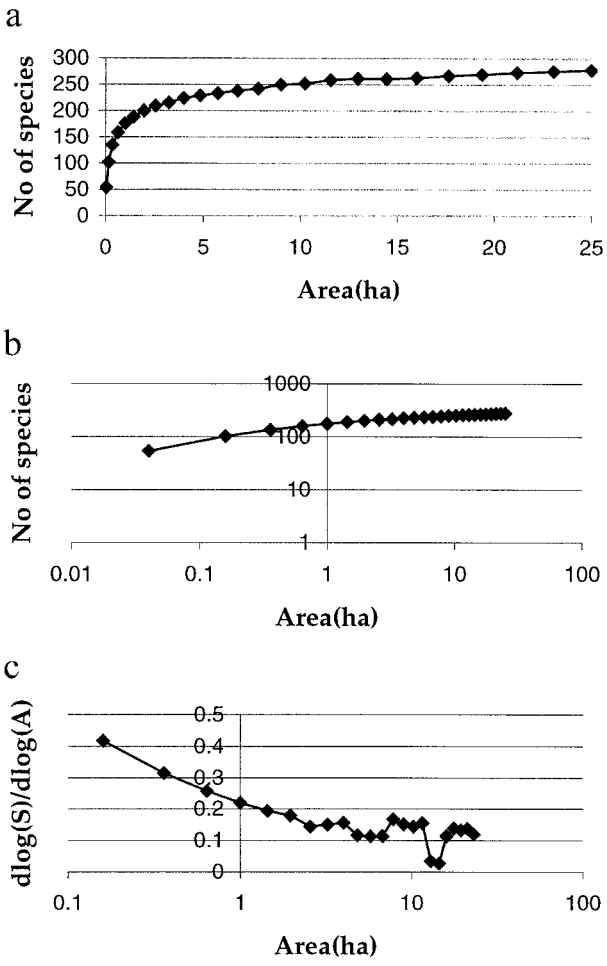

Figure 2: *a*, Species-area relationship. The area of the left-most point is $(1 \times 1) \times 25$ m^2; the area of the second left-most point is $(5 \times 5) \times 25$ m^2; the area of the of the third left-most point is $(9 \times 9) \times 25$ m^2, etc. *b*, SAR plotted in logarithmic scales. *c*, Derivative of the curve in *b* obtained by the central-difference method.

Sample Application of Multifractals

Study Site and Methods

We illustrate the application of the method of moments and of the histogram method to a data set on tree and shrub species in a rectangular, 50-ha plot (1,000 m^2 × 500 m^2) of old-growth tropical moist forest on Barro Colorado Island (BCI), Panama (Condit et al. 1992). The

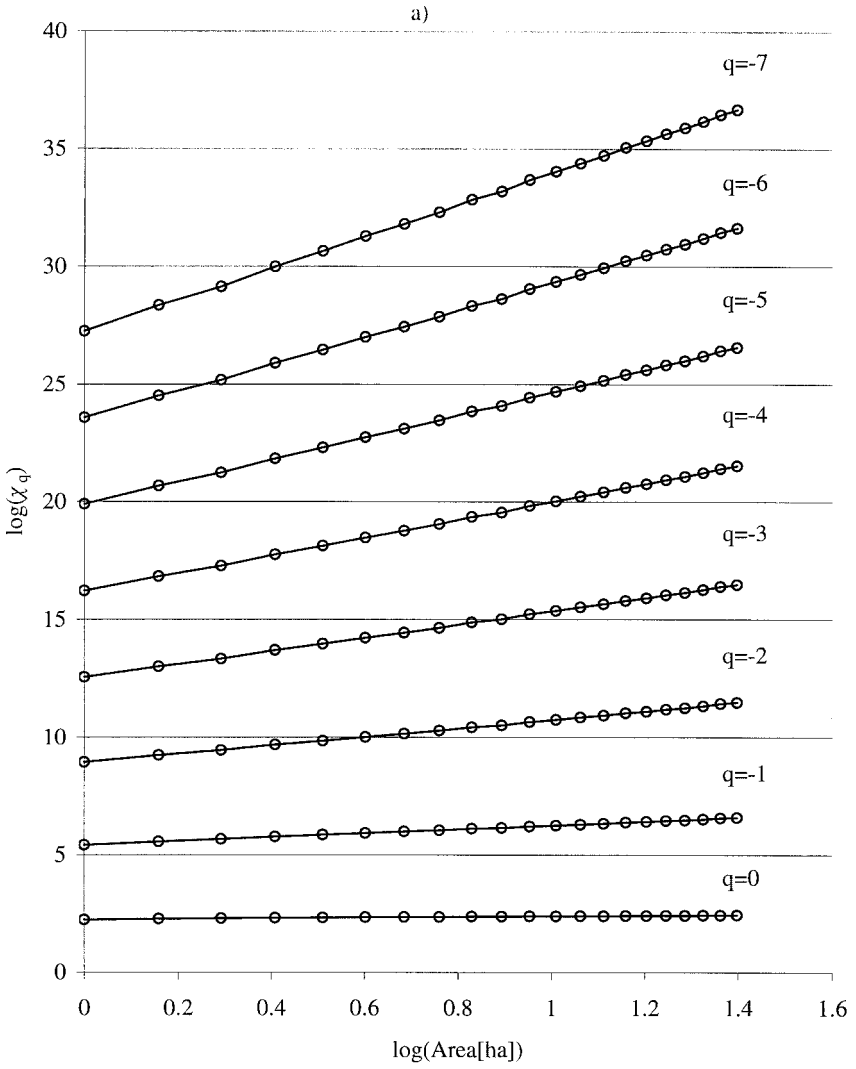

Figure 3*a*: $\log(X_q)$ as a function of the $\log(A)$ for some integer values of $q \leq 0$

BCI data set contains information on the spatial coordinates and diameter at breast height (dbh) of all woody plants (with exception of lianas) with stem diameter ≥ 1 cm dbh, collected in five different census (1982, 1985, 1990, 1995, 2000). For the purposes of this article, we present results for only the 1982 census since results were similar for all the other censuses. The 1982 data set contains records on 305 species and about 235,000 individual stems.

Previously, Manrubia and Solé (1996) and Solé and Manrubia (1995*a*, 1995*b*) have applied multifractals to the analysis of the 50-ha-plot BCI data, but their work concerned a different topic—the spatial distribution of gaps. Here, we deal with data on species composition and relative abundance.

In the previous section, we indicated that the method of moments is not always applicable, but when it is, convergence tends to be faster than with the histogram method, which is then preferable. For this reason, we first analyze the data using the method of moments.

Recall that the method of moments directly leads to the spectrum of generalized exponents, z_q (eq. [8]). In order to determine the number of species, $S(A)$, and their relative abundance, p_i, for different area sizes, A, we used a procedure suggested by Rosenzweig (1995, p. 9) to determine the SAR. First, divide the 50-ha plot into smaller, nonoverlapping squared subplots; the largest subplot is 500 m^2 × 500 m^2 and the smallest is 20 m^2 × 20 m^2. All subplots have the same (square) shape. For each subplot of area A, the number of species, $S(A)$, and their relative

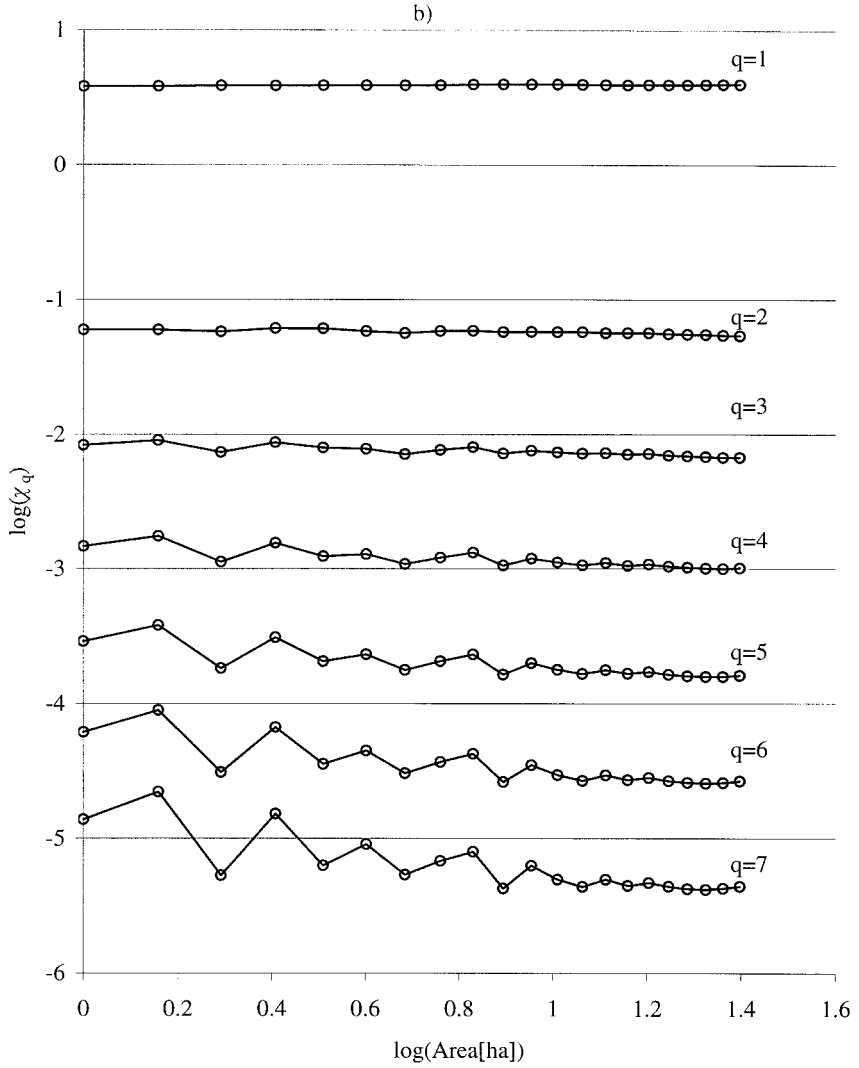

Figure 3*b*: Same for some integer values of $q \geq 1$

abundances, p_i, were determined, and from these, the partition function $\chi_q = \sum_{i=1}^{S(A)} p_i^q$ (eq. 7) was calculated. We then averaged the values of χ_q of all the subplots with the same area (see Mandelbrot [1988] for a discussion of the implications of the averaging process). This means that equation (8) should be instead rewritten as

$$z_q = \lim_{A \to \infty} \frac{1}{1-q} \frac{\log\left(\left\langle \sum_{i=1}^{S(A)} p_i^q \right\rangle\right)}{\log(A)}, \qquad (17)$$

where the angle brackets denote average.

Statistical Issues

Before proceeding further, a statistical caveat is necessary. The method adopted here is one that uses nested sample areas; that is, data collected in smaller-area samples also contribute to the larger-area samples (Leitner and Rosenzweig 1997). This implies that data from different samples are not independent. In fact, even if the nested design had been avoided, the data might still exhibit some spatial dependence (spatial autocorrelation) because, on average, we would expect quadrates that are closer together to be more similar than ones further apart (Palmer and White 1994). The method of moments requires fitting straight

lines to these data. This is usually done using least squares regression methods (e.g., Morse et al. 1985; Cheng and Agterberg 1995), and we have followed this convention here. However, it should be noted that the lack of independence in the data violates the usual assumptions underlying linear regression. Therefore, we use the coefficient of determination, R^2, as simply a descriptive measure of goodness of fit. The coefficient R^2 can be calculated as

$$R^2 = 1 - \frac{\sum (Y_i - \hat{Y}_i)^2}{\sum (Y_i - \overline{Y}_i)^2},$$

where the numerator is the sum of squared deviations from the fitted model, and the denominator is the sum of squared deviations from the mean.

The SAR of the BCI 50-ha Plot

Returning to the estimation of the z_q spectrum, a necessary though not sufficient condition for a species abundance distribution to be multifractal is that the SAR is reasonably described by a power law. This can be verified by plotting the SAR on a log-log plot and observing whether it is approximately a straight line within a range of areas (the scaling region). Over all spatial scales, the SAR is actually triphasic (Rosenzweig 1995; Hubbell 2001). For small areas, the SAR is a decelerating curve on a log-log plot; that is, it has a negative second derivative; for intermediate values of area, it is approximately a straight line; that is, a power law is a good approximation; and for large areas, a new power law with a higher value of z is observed, approaching a slope of unity at very large spatial scales. The triphasic nature of these curves has been explained by Hubbell (1997, 2001) as follows. On local spatial scales, the species accumulation curve is very sensitive to relative species abundance: common species are collected quickly, and then rarer species are added more slowly. On intermediate spatial scales, a log-log linear region arises from the sampling of species ranges at equilibrium between speciation, dispersal, and extinction over the biogeographic region. At very large scales, the correlation length of the geographic processes is exceeded, beyond which sampling of regions with independent evolutionary and biogeographic histories occurs. Durrett and Levin (1996) predict a limiting slope of unity as the large-area sample units become dynamically uncoupled and independent. Thus, the intermediate and large areas correspond to two different scaling regions. An important point needs to be made here: the existence of different scaling regions should not be confused with multifractality. If more than one scaling region is observed, then each of these regions may hold a distinct multifractal distribution.

The SAR curve is plotted in figure 2*a* and 2*b* on both linear and logarithmic scales, respectively, for the BCI data census of 1982 using all individuals larger than 1 cm dbh. Visual inspection of the curve of figure 2*b* reveals that it is slightly curved downward, a result already reported by Condit et al. (1996) and in agreement with the previous discussion on the shape of the SAR for small areas. What remains to be investigated is whether for larger areas a power law is a good approximation for the SAR of the BCI tree community.

As mentioned, there are no theoretical methods to specify the limits of the scaling region. In order to determine whether the curve of figure 2*b* is approximately straight in some region of the range of areas available in the 50-ha plot, that is, whether a scaling region exists, the derivative of this curve was calculated by the central-difference method. The justification of this procedure is as follows: if there is a region of the plane where the curve is approximately linear, then the derivative should be approximately constant in that region. Results are shown in figure 2*c*: for small values of A, the slope decreases, indicating that for these values of A, a power law is not a reasonable approximation for the SAR. However, for $A \geq 1$ ha, the slope of the majority of the points falls between 0.1 and 0.2. Linear regression of the points above 1 ha gave a value of $z_0 = 0.136$, $R^2 = 0.994$, indicating that the SAR is well approximated by a power law. The ratio of the largest area, 25 ha, to the smallest area, 1 ha, is slightly above one order of magnitude.

The Method of Moments

Once a scaling region has been identified the method of moments requires the determination of the curves of $\log(\langle \sum_{i=1}^{S(A)} p_i^q \rangle)$ versus $\log(A)$ or $\langle \sum_{i=1}^{S(A)} p_i \log(p_i) \rangle$ versus $\log(A)$ for $q = 1$, within the same range of areas used to estimate z_0. Values of q between $-7 < q < 7$ were used because, for very large positive or very small negative q, values of p_i^q become too extreme in size to be handled by the computer. These curves are shown in figure 3*a* for integer values of $q \leq 0$ and in figure 3*b* for $q \geq 1$. The slopes, τ_q, calculated by least squares, are shown in table 1, together with the respective R^2. As can be observed, very good fits were obtained for $q < 1$, but the fit suddenly deteriorates for $q > 1$. The spectrum of the generalized exponents, $z_q = (1 - q)\tau_q$, is shown in figure 4. Notice that for approximately $q > 1$, z_q increases, contrary to theoretical predictions, which assert that z_q should be a monotonically decreasing function of q. The anomalous increase in the z_q spectrum turned out to be very persistent in the BCI case, even when other techniques were considered. It did not disappear when the curves were interpolated by nonlinear (quadratic) regression or when subplots of dif-

ferent areas were spatially arranged so that they were not nested.

These results are intriguing. One possible explanation is that z_q is not defined for $q > 1$ since it is for this range of q that the fit is worse, a situation that would occur if the relative abundance of at least one species decays to zero as a function of area slower than any negative power law (as discussed in the previous section). If this is the case, then it is likely that similar results will be found for other data on trees and shrubs collected in 50-ha plots in other tropical forests. However, we think it is premature to conclude much about the characteristics of the multifractal spectrum because of the small range of areas A (only approximately one order of magnitude). It is possible that if data from larger areas were available, the trend observed in D_q for positive q would have been reversed. It is also possible that if plants with dbh smaller than 1 cm had been sampled the results would have been different. However, it is worth mentioning that the qualitative shape of the species abundance distributions for the BCI plot are largely invariant with changes in cutoff diameter of the census. For example, they are very similar with larger cutoff diameters; published distributions for 10- and 20-cm-dbh-size class cutoffs for the BCI plot can be found in Hubbell (2001) and in Hubbell and Foster (1983), showing the qualitative invariance of the curves. We do not know what the distributions would be if all seedlings and saplings <1 cm were included. However, the census of all plants >20 cm dbh in 20,000 one-square-seedling quadrates over the entire 50-ha plot is currently being carried, which should give us a better estimate of the curve for the entire plant community.

The Histogram Method

We now illustrate the application of the histogram method with the renormalization given by equation (15). The histogram method converges slowly, given the small range of the scaling region on BCI, so it is unlikely that the collapse of the preasymptotic $f_A(\alpha)$ curves into a single curve will be observed. Nevertheless, because the histogram method makes use of the full distribution function for each value of A, it has the merit of showing the preasymptotic curves, $f_A(\alpha)$, giving some clues to the possible shape of the $f(\alpha)$ spectrum, which was not possible with the method of moments because of the problems observed for positive q.

As before, the 50-ha plot was divided into squares ranging from 1 to 25 ha in size. For each sample of area A, the relative abundance of each species, p_i, was calculated, as well as the respective Hölder exponent, $\alpha_i = -\log(p_i)/\log(A)$. The observed range of α values ($0.13 \leq \alpha \leq 0.94$) was then divided into 16 bins, with size $\Delta\alpha = 0.05$, and the number of occurrences in each bin was determined. If the number of occurrences in a bin, α', is S_b, then $S_b/\Delta\alpha$ is an approximation of S_α. The final histogram of the number of species, S_α, as a function of α for a given area A was obtained by taking the average of all histograms of the subplots with the same area A. Note that this process may lead to noninteger values of S_α and, in particular, to $S_\alpha < 1$. We are not interested in the number of species in each bin but, rather, in the log of this number divided by $\log(A)$. For each histogram, the log of the number of species in each bin was taken followed by division by $\log(A)$. The curves obtained by this process correspond to $f_A(\alpha)$. Preasymptotic $f_A(\alpha)$ curves for five different values of A (1, 4, 9, 16, 25 ha) are shown in figure 5*a*–5*e*. The negative values of $f_A(\alpha)$ result from the averaging process used to obtain these curves.

A striking feature in these plots is that the underlying distributions are not lognormal. If they were, the curves would have been symmetric relative to the maximum and shaped like a negative quadratic polynomial ($-x^2$). The curve that comes closest to this shape is the one corresponding to the smallest area (1 ha; fig. 5*a*), although with a truncated right side; all the other curves exhibit a clear right fat tail. Since the right-hand side of the $f_A(\alpha)$ curves corresponds to the rarest species, this result demonstrates that when the area increases, the number of rare species observed increases considerably. The nonlognormality of the species abundance curve of this tree community is not a new result (see, e.g., Hubbell 1997, 2001). Here, however, we show this result for different areas. Interestingly, we also reproduce a well-known result: the approximate lognormality observed for small sample sizes is not observed when the sample sizes increase (see also discussion in the next section).

Table 1: Slopes (τ_q), respective generalized exponent (z_q), and coefficients of determination (R^2) for integer values of q

q	τ_q	z_q	R^2
−7	6.808	.851	.999
−6	5.826	.832	.999
−5	4.842	.807	.999
−4	3.854	.770	.999
−3	2.860	.714	.998
−2	1.858	.619	.997
−1	.861	.430	.996
0	.136	.136	.988
1	−.012	.048	.788
2	−.033	.033	.421
3	−.082	.041	.450
4	−.159	.053	.515
5	−.260	.065	.564
6	−.381	.076	.600
7	−.520	.086	.626

Note: Data obtained from the 1982 BCI census.

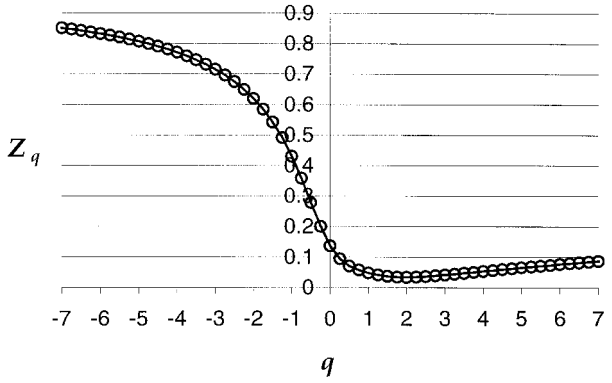

Figure 4: The spectrum of generalized exponents z_q

Figure 6 shows the previous preasymptotic $f_A(\alpha)$ curves on a single graph. The figures were vertically shifted to make all the maxima coincide at zero. The heights of the different curves are not important; what matters is the shape of the curves (Evertsz and Berkner 1995). Visual inspection of theses curves does not give unequivocal evidence for convergence of the $f_A(\alpha)$ curves. To assess the similarity of the shapes of the preasymptotic $f_A(\alpha)$, we plotted the absolute difference between the curves of two consecutive area sizes in figure 7.

Figure 7 shows a clear decrease in the absolute difference between $f_A(\alpha)$ curves of the smallest area sizes. In particular, note the constant decrease in the difference between curves for the three smallest values of α, the region corresponding to the most abundant species.

To quantify the difference between curves, we computed the total sum of the difference between two $f_A(\alpha)$ of two area sizes, A' and A'', according to

$$|\Delta f_A(\alpha)| = \sum_{\alpha_i=\alpha_{\min}}^{\alpha_{\max}} |f_{A''}(\alpha_i) - f_{A'}(\alpha_i)|.$$

Results are shown in table 2. This table reveals an initially rapid decline in the difference between the curves corresponding to the two smallest areas, followed by smaller for the curves of the larger areas. The difference between the 16- and 9-ha curves is slightly above the one of the 9- and 4-ha curves. Notice that the smallest difference between two curves is observed for the two largest areas, suggesting that the curves are slowly converging.

These first results are encouraging. Nevertheless, much more work is required to access the multifractality of the species abundance distribution function, and in particular, there is much scope to improve some of the methods exemplified here. We believe that as larger sample areas become available in the future, we will find stronger ev-

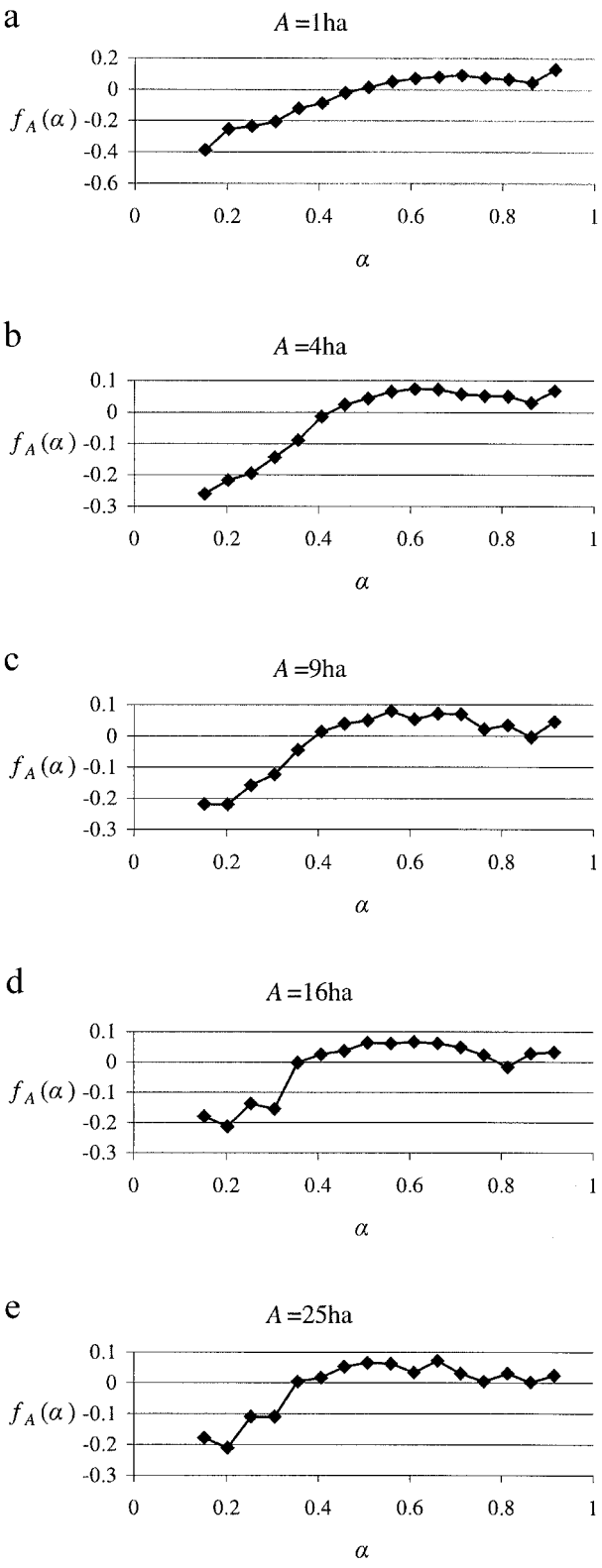

Figure 5: Histograms of the preasymptotic $f_A(\alpha)$ curves for area = 1, 4, 9, 16, and 25 ha.

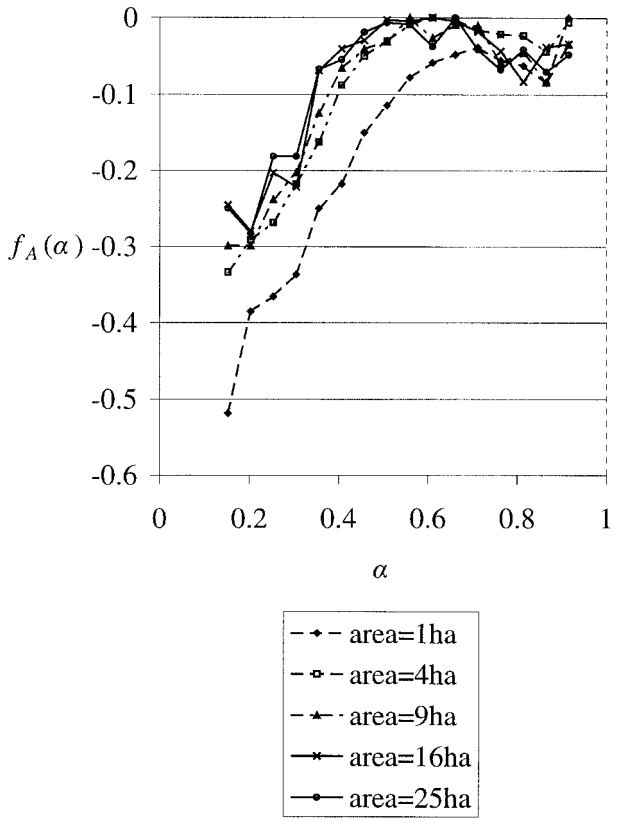

Figure 6: Histograms of $f_A(\alpha)$ for different values of the area. To help comparison, the maximums were vertically shifted to zero.

idence of the multifractal pattern suggested. In any case, application of multifractal methods to species abundance distributions is likely to elucidate the characteristics of the underlying species distributions.

Implications

There are a number of uses and implications of the theory of multifractals for the description and measurement of diversity in ecology. The two approaches to multifractals, the method of moments and the histogram method, highlight different aspects of diversity, SARs, and relative species abundance patterns. We start with the method of moments.

One of the most interesting results of the multifractal method of moments is that it predicts a power-law scaling relationship between the Shannon, the Simpson, and the Berger-Parker diversity indices and area (eqq. [10]–[12]). We encourage testing the prediction of such a scaling relationship on a wide range of taxonomic groups in distinct biomes. If the power-law scaling with area is observed, then it is possible to extrapolate the value of the Shannon, Simpson, and Berger-Parker diversity indices to larger areas, at least where the power-law SAR holds. It should be noted that these indices were derived in the positive range of q (see eq. [8]), where, at least for the BCI data, the poorer fits to a power law were observed. We repeat that it is premature to speculate how general this result is (i.e., poor fit to power laws observed in the positive range of q among ecological communities).

The power-law relationship between the Shannon and the Simpson indices and area may not be confined to the species level. In fact, data collected by E. Guilbert (1998, personal communication) on arthropod communities of New Caledonia show at the family level that the Shannon and the Simpson indices ($q = 1$ and $q = 2$, respectively) do exhibit a power-law relationship above a certain area. It remains to be tested whether power laws are observed for Guilbert's data for other smaller and larger values of q. The absence of a theoretical formalism relating the above diversity indices and area, such as the one given by equation (8), may be the reason why the power-law scaling of these indices has not been reported.

Another important insight given by the method of moments is the relationship between population density and range size implied by equation (8). A positive relationship between range and abundance is well documented in the literature (e.g., Brown 1984; Gaston et al. 1997). Equation (8) accommodates for such a positive relationship. To understand why range and abundance are correlated, consider the extreme situations of $q \to -\infty$ and $q \to +\infty$, which correspond to the least and most abundant species, respectively. According to equations (12) and (13)

$$p_{\min} \propto A^{-z_{-\infty}},$$

$$p_{\max} \propto A^{-z_{-\infty}}.$$

Since $z_{-\infty} \geq z_{+\infty}$, these equations imply that the relative abundance of the rarest species decays faster with area than the relative abundance of the most abundant species. One possibility for this is that rare species have smaller ranges than abundant species. However, one can imagine a species that is rare everywhere but extremely widespread at low density, but the evidence to date suggests that species such as these are few, if any (e.g., Rabinowitz et al. 1986; Pitman et al. 1999). More generally, the shape of the z_q spectrum (a monotonically decreasing function of q) implies a functional relationship between the species abundance and range—recall that in the limit $A \to \infty$, each value of q selects a particular value of p_i—compatible with the fact that more abundant species have larger ranges.

The importance of the relationship between species abundance and range should not be underestimated for understanding the observed values of z_0, although it was

not part of the original theories of Preston (1962) and May (1975). Leitner and Rosenzweig (1997) and Pelletier (1999) have shown that in order to obtain z values close to those empirically observed, one has to introduce a functional relationship between abundance and range. Pelletier (1999, p. 1984) considered that "the population density of individuals in a species [...] is an uncorrelated random variable with variance $V \propto (N/A)^{3/2}$, where N/A is the mean population density," while Leitner and Rosenzweig (1997) assumed a power-law relationship between population density and range. The work by Leitner and Rosenzweig (1997) is particularly relevant since it showed that assuming simply that the range size is a linear function of abundance led to z values close to 0.77, much higher than those empirically observed. What the multifractal formalism brings to this discussion is a relationship between the fraction of individuals of a species p_i and area A, which is not an extra assumption but one that arises out of the multifractal theory applied to the power-law SAR.

The shape of the species abundance distributions and the effect of sample size have been another pervasive theme in ecological studies (e.g., Nee et al. 1991). The histogram method, by dealing directly with the species abundance distributions at different spatial scales, can give important insights into this question. Fisher et al. (1943) first suggested that the species abundance distribution could be approximated by a log series. Later, Preston (1948) noticed that the log series did not fit most of his data. Preston (1948) argued that the difference observed in the shape of the abundance distributions was an artifact of the sample size and, in particular, that the log series observed by Fisher et al. (1943) was due to relatively small data sets. Preston (1948) pointed out that when larger samples were collected, a lognormal distribution would be a better approximation of the species abundance distribution. He also noticed that the observed abundance distributions were truncated lognormal curves that lacked the least abundant species. Preston (1948) predicted that if larger samples were collected, the omitted left side of the distributions, corresponding to rare species, would be revealed. More recently, however, abundance distributions obtained with larger sets (e.g., Gibbons et al. 1993; Gregory 1994; Hubbell 1997, 2001) have failed to confirm Preston's prediction. In general, these abundance distributions have more rare species than allowed by the symmetrical log-transformed–lognormal distribution. These observations have led several authors to challenge the assumption of lognormality (e.g., Nee et al. 1991; Hubbell 1997, 2001; Harte et al. 1999). An important aspect of the multifractal theory is that it does not require a lognormal distribution (e.g., Mandelbrot and Evertsz 1996), and it accommodates distributions with long tails for rare species as observed in real data sets. However, probably the most important insight from multifractals on this issue is to show that the species abundance distributions obtained at different areas, after renormalization, should collapse into a single curve. This result has far-reaching consequences, in particular, for measurements of species diversity and conservation studies because once multifractality has been established it allows one to extrapolate the species abundance distribution to larger areas where the power-law SAR is observed. So far, studies have only attempted to extrapolate species richness (e.g., Palmer 1990; Baltanás 1992; Colwell and Coddington 1994).

If there are scaling laws, not only for species richness but also for relative species abundance as a function of

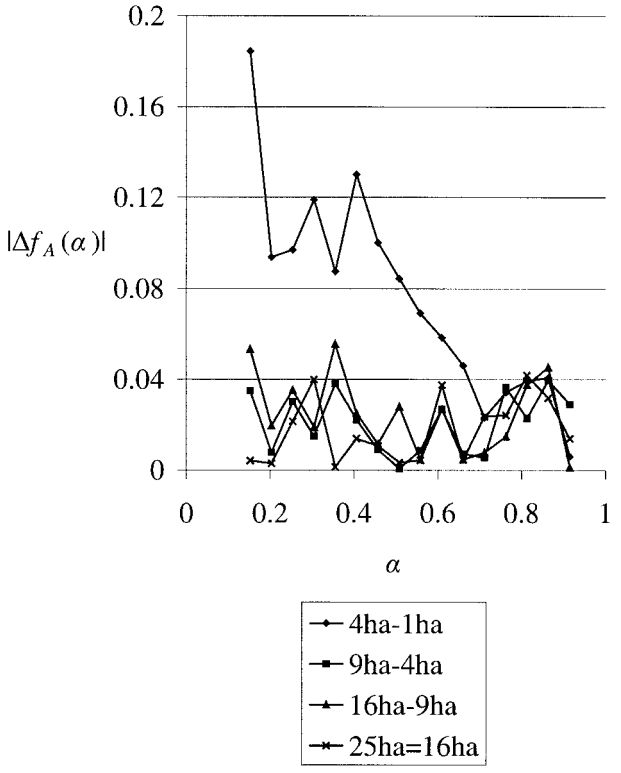

Figure 7: Absolute difference between preasymptotics, $f_A(\alpha)$, of consecutive areas.

Table 2: Total absolute difference of the $f_A(\alpha)$ curves of two consecutive area sizes

Areas (ha)	$\Delta f_A(\alpha)$
4–1	1.214
9–4	.337
16–9	.390
25–16	.280

area, or if the distribution of relative species abundance collapses after appropriate transformations, then both observations could be of immense practical utility for estimating biodiversity on larger spatial scales than can be reasonably or economically sampled. Whether these theoretical promises will be borne out in practice remains to be seen.

Summary

We have applied the theory of multifractals to the dual problems of the SAR and relative species abundance. The application of multifractal methods was illustrated with data on tropical trees and shrubs in a tropical forest in Barro Colorado Island, Panama. The results of this application suggest that wider testing of multifractal theory is warranted on similar but larger areas and data sets. Our analysis suggests the exciting and potentially far-reaching conclusion that predictive scaling relationships exist, not only for species-area curves but also for relative species abundance on large spatial scales. Such scaling laws could be of considerable value. These scaling laws may reveal further laws, hitherto unsuspected, for how ecological communities are assembled on local-to-landscape spatial scales. These scaling laws also can be used as benchmark criteria for evaluating the performance of mechanistic simulation models that attempt to recreate SARs and patterns of relative species abundance.

Acknowledgments

We thank Julian Evans, Harold M. Hastings, Ann P. Kinzig, Geoffrey Kirkwood, and John Lawton for their careful reading and valuable comments and suggestions on this article and J. Harte and J. N. Elgin for stimulating discussions. We thank E. Guilbert for making available unpublished data. L.B.A. thanks Pablo Inchausti for pointing out the previous work by M. O. Hill and the Fundação para a Ciência e Tecnologia for financial support. S.P.H. thanks the National Science Foundation, the Smithsonian Tropical Research Institute, and numerous private foundations for support of both his theoretical and empirical work on and off Barro Colorado Island.

APPENDIX

The Relation between the $f(\alpha)$ and the z_q Spectra

The partition function, $\chi_q(A)$ (eq. [7]), can be written in terms of the Hölder exponent (eq. [14]) as

$$\chi_q(A) = \sum_{i=1}^{S(A)} (A^{-\alpha_i})^q = \sum_{j=\alpha_{\min}}^{\alpha_{\max}} (A^{-q\alpha_j}) S_{\alpha_j}(A), \qquad \text{(A1)}$$

where $S_{\alpha_j}(A)$ is the number of species with exponent α_j within area A; this is a transformation similar to the one between equations (4) and (5). If α is a quasi-continuous variable, then the contribution to the sum from species with α between α and $\alpha + d\alpha$ is

$$S_{\alpha_j}(A)(A^{-q\alpha})d\alpha.$$

If $0 < \alpha_{\min} < \alpha < \alpha_{\max} < \infty$, the sum in the partition function can be replaced by the following integral

$$\chi_q(A) = \int_{\alpha_{\min}}^{\alpha_{\max}} S_{\alpha_j}(A)(A^{-q\alpha})d\alpha. \qquad \text{(A2)}$$

Making use of equation (15), the number of species can be written in terms of the scaling exponents $f(\alpha)$ as

$$S_{\alpha_j}(A) \propto A^{f(\alpha)}.$$

Substitution of the previous equation into equation (A2) leads to

$$\chi_q(A) \propto \int_{\alpha_{\min}}^{\alpha_{\max}} A^{[f(\alpha)-q\alpha]} d\alpha. \qquad \text{(A3)}$$

To solve the previous integral, we make the following approximation: since $A \to +\infty$, the value of the integral is close to the contribution from the value of α that maximizes $[f(\alpha) - q\alpha]$. That is, for a given q,

$$\left\{\frac{d}{d\alpha}[f(\alpha) - q\alpha]\right\}_{\alpha=\alpha(q)} = 0,$$

or

$$\left.\frac{df(\alpha)}{d\alpha}\right|_{\alpha=\alpha(q)} = q, \qquad \text{(A4)}$$

and, since we require the extreme to be a maximum,

$$\left.\frac{d^2[f(\alpha) - q\alpha(q)]}{d\alpha^2}\right|_{\alpha=\alpha(q)} < 0,$$

or

$$\left.\frac{d^2 f(\alpha)}{d\alpha^2}\right|_{\alpha=\alpha(q)} < 0.$$

The last equation shows that the $f(\alpha)$ curve is necessarily cap convex, and equation (A4) shows that the maximum of this curve occurs for $q = 0$.

Keeping only the value of $\alpha(q)$ that gives the maximum contribution to the integral, equation (A3) can be written as

$$\chi_q(\alpha) \propto A^{f(\alpha(q))-q\alpha(q)}.$$

From equation (8), we can say that

$$\chi_q(\alpha) \propto A^{(1-q)z_q}.$$

Then, comparing the two previous equations,

$$(1 - q)z_q = f(\alpha(q)) - q\alpha(q). \quad \text{(A5)}$$

The last equation relates the spectra of z_q and $f(\alpha)$. In addition, a relation between $\alpha(q)$ and z_q can be obtained by taking the derivative of equation (A5) in order to q and making use of equation (A4). The result is

$$\alpha(q) = z_q - (1 - q)\frac{dz_q}{dq}. \quad \text{(A6)}$$

The pair of equations (A5) and (A6) is a Legendre transformation, and it allows the calculation of the spectrum $f(\alpha)$ once z_q is obtained and vice versa.

Literature Cited

Arrhenius, O. 1921. Species and area. Journal of Ecology 9:95–99.

Baltanás, A. 1992. On the use of some methods for the estimation of species richness. Oikos 65:484–492.

Brown, J. H. 1984. On the relationship of distribution and abundance of species. American Naturalist 124: 255–279.

Caswell, H., and J. E. Cohen. 1993. Local and regional regulation of species-areas relations: a patch-occupancy model. Pages 99–107 *in* R. E. Ricklefs and D. Schluter, eds. Species diversity in ecological communities. University of Chicago Press, Chicago.

Cheng, Q., and F. P. Agterberg. 1995. Multifractal modeling and spatial point processes. Mathematical Geology 27: 831–845.

Colwell, R. K., and J. A. Coddington. 1994. Estimating terrestrial biodiversity through extrapolation. Philosophical Transactions of the Royal Society of London B, Biological Sciences 345:101–118.

Condit, R., S. P. Hubbell, and R. B. Foster. 1992. Short-term dynamics of a Neotropical forest. BioScience 42: 822–828.

Condit, R., S. P. Hubbell, J. V. Lafrankie, R. Sukumar, N. Manorakan, R. B. Foster, and P. S. Ashton. 1996. Species-area and species-individual relationships for tropical trees: a comparison of three 50-ha plots. Journal of Ecology 84:549–562.

Durrett, R., and S. Levin. 1996. Spatial models for species-area curves. Journal of Theoretical Biology 179:119–127.

Evertsz, C. J. G., and K. Berkner. 1995. Large deviation and self-similarity analysis of graphs: DAX stock prices. Chaos, Solitons and Fractals 6:121–130.

Evertsz, C. J. G., and B. B. Mandelbrot. 1992. Multifractal measures. Pages 921–953 *in* H.-O. Peitgen, H. Jürgens, and D. Saupe, eds. Chaos and fractals: new frontiers of science. Springer, New York.

Fisher, R. A., A. S. Corbet, and C. B. Williams. 1943. The relation between the number of species and the number of individuals in a random sample of an animal population. Journal of Animal Ecology 12:42–58.

Gaston, K. J., T. M. Blackburn, and J. H. Lawton. 1997. Interspecific abundance-range size relationships: an appraisal of mechanisms. Journal of Animal Ecology 66: 579–601.

Gibbons, D. W., J. B. Reid, and R. A. Chapman. 1993. The new atlas of breeding birds in Britain and Ireland, 1988–1991. Poyser, London.

Gilpin, M. E., and J. M. Diamond. 1980. Subdivision of nature reserves and the maintenance of species diversity. Nature 285:567–568.

Grassberger, P. 1983. Generalized dimensions of strange attractors. Physics Letters 97A:227–230.

Gregory, R. 1994. Species abundance patterns of British birds. Proceedings of the Royal Society of London B, Biological Sciences 257:299–301.

Guilbert, E. 1998. Studying canopy arthropods in New Caledonia: how to obtain a representative sample. Journal of Tropical Ecology 14:665–672.

Halsey, T. C., M. H. Jensen, L. P. Kadanoff, I. Procaccia, and B. I. Shraiman. 1986. Fractal measures and their singularities: the characterization of strange sets. Physical Review A 33:1141–1151.

Harte, J., and A. P. Kinzig. 1997. On the implications of species-area relationships for endemism, spatial turnover, and food web patterns. Oikos 80:417–427.

Harte, J., A. Kinzig, and J. Green. 1999. Self-similarity in the distribution and abundance of species. Science (Washington, D.C.) 284:334–336.

Hastings, H. M., and G. Sugihara. 1993. Fractals: a user's guide for the natural sciences. Oxford University Press, Oxford.

Higgs, A. J., and M. B. Usher. 1980. Should nature reserves be large or small? Nature 285:568–569.

Hill, M. O. 1973. Diversity and evenness: a unifying notation and its consequences. Ecology 54:427–432.

Hubbell, S. P. 1997. A unified theory of biogeography and relative species abundance and its application to tropical rain forests and coral reefs. Coral Reefs 16(suppl.): S9–S21.

———. 2001. The unified neutral theory of biodiversity and biogeography. Princeton University Press, Princeton, N.J.

Hubbell, S. P., and R. B. Foster. 1983. Diversity of canopy trees in a Neotropical forest and implications for the conservation of tropical trees. Pages 25–41 *in* S. J. Sutton, T. C. Whitmore, and A. C. Chadwick, eds. Tropical rain forests: ecology and management. Blackwell, Oxford.

Leitner, W. A., and M. L. Rosenzweig. 1997. Nested species-area curves and stochastic sampling: a new theory. Oikos 79:503–512.

MacArthur, R. H., and E. O. Wilson. 1967. The theory of island biogeography. Princeton University Press, Princeton, N.J.

Magurran, A. E. 1988. Ecological diversity and its measurement. Princeton University Press, Princeton, N.J.

Mandelbrot, B. B. 1988. A class of multinomial multifractal measures with negative (latent) values for the "dimension" $f(\alpha)$. Pages 3–29 *in* L. Pietronero, ed. Fractals: physical origin and properties. Plenum, New York.

Mandelbrot, B. B., and C. J. G. Evertsz. 1996. Exactly self-similar left-sided multifractals. Pages 359–399 *in* A. Bunde and S. Havlin, eds. Fractals and disordered systems. 2d ed. Springer, Berlin.

Manrubia, S. C., and R. V. Solé. 1996. Self-organized criticality in rainforest dynamics. Chaos, Solitons and Fractals 7:523–541.

May, R. M. 1975. Patterns of species abundance and diversity. Pages 81–120 *in* M. L. Cody and J. M. Diamond, eds. Ecology and evolution of communities. Harvard University Press, Cambridge, Mass.

May, R. M., J. H. Lawton, and N. E. Stork. 1995. Assessing extinction rates. Pages 1–24 *in* J. H. Lawton and R. M. May, eds. Extinction rates. Oxford University Press, Oxford.

Morse, D. R., J. H. Lawton, M. M. Dobson, and M. H. Williamson. 1985. Fractal dimension of vegetation and the distribution of arthropod body lengths. Nature 314: 731–733.

Nee, S., P. H. Harvey, and R. M. May. 1991. Lifting the veil on abundance patterns. Proceedings of the Royal Society of London B, Biological Sciences 243:161–163.

Ney-Nifle, M., and M. Mangel. 1999. Species-area curves based on geographic range and occupancy. Journal of Theoretical Biology 196:327–342.

Paladin, G., and A. Vulpiani. 1987. Anomalous scaling laws in multifractal objects. Physics Reports 156:147–225.

Palmer, M. W. 1990. The estimation of species richness by extrapolation. Ecology 71:1195–1198.

Palmer, M. W., and P. S. White. 1994. Scale dependence and the species-area relationship. American Naturalist 144:717–740.

Pascual, M., F. A. Ascioti, and H. Caswell. 1995. Intermittency in the plankton: a multifractal analysis of zooplankton biomass variability. Journal of Plankton Research 17:1209–1232.

Pelletier, J. D. 1999. Species-area relation and self-similarity in a biogeographical model of speciation. Physical Review Letters 82:1983–1986.

Pimm, S. L., G. J. Russell, J. L. Gittleman, and T. M. Brooks. 1995. The future of biodiversity. Science (Washington, D.C.) 269:347–350.

Pitman, N. C. A., J. Terborgh, M. R. Silman, and V. Percy Nunez. 1999. Tree species distributions in an upper Amazonian forest. Ecology 80:2651–2661.

Preston, F. W. 1948. The commonness, and rarity, of species. Ecology 29:254–283.

———. 1962. The canonical distribution of commonness and rarity. I. Ecology 43:182–215.

Rabinowitz, D., S. Cairns, and T. Dillon. 1986. Seven forms of rarity and their frequency in the flora of the British Isles. Pages 182–204 *in* M. E. Soulé, ed. Conservation biology: the science of scarcity and diversity. Sinauer, Sunderland, Mass.

Rényi, A. 1961. On measures of entropy and information. Pages 547–561 *in* J. Neyman, ed. 4th Berkeley Symposium on Mathematical Statistics and Probability. University of California Press, Berkeley.

Rosenzweig, M. L. 1995. Species diversity in space and time. Cambridge University Press, Cambridge.

Solé, R. V., and S. C. Manrubia. 1995*a*. Are rainforests self-organized in a critical state? Journal of Theoretical Biology 173:31–40.

———. 1995*b*. Self-similarity in rain forests: evidence for a critical state. Physical Review E 51:6250–6253.

Associate Editor: Lewi Stone